$\mu \to e$ conversion in nuclei and nuclear charge distributions

Frederic Noël

Universität Bern
Institute for Theoretical Physics

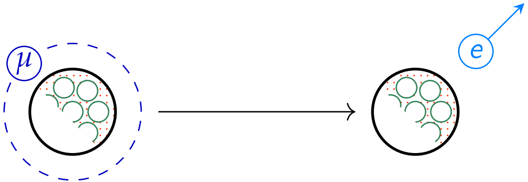

01.10.2024

Workshop: Exploring BSM physics with muons

[Hoferichter, Menéndez, Noël; Phys. Rev. Lett. 130 (2023)]
[Noël, Hoferichter; JHEP 08 (2024)]
[Heinz, Hoferichter, Miyagi, Noël, Schwenk; in preparation]

Lepton Flavour Violation

- Search for new physics (NP):
  one prominent probe $\rightarrow$ LFV

Lepton Flavour Violation

- Search for new physics (NP):
  one prominent probe $\rightarrow$ LFV
- Lepton Flavour (LF) is conserved by SM
- LF is an (accidental) global symmetry

Lepton Flavours

e	μ	τ
ν_e	ν_μ	ν_τ

Lepton Flavour Violation

- Search for new physics (NP):
  one prominent probe → LFV
- Lepton Flavour (LF) is conserved by SM
- LF is an (accidental) global symmetry

- Lepton Flavour Violation (LFV)
  - neutral LFV: ν_e, ν_μ, ν_τ
    → neutrino oscillations

Lepton Flavours

e	μ	τ
ν_e	ν_μ	ν_τ

Lepton Flavour Violation

- Search for new physics (NP):
  one prominent probe $\rightarrow$ LFV
- Lepton Flavour (LF) is conserved by SM
- LF is an (accidental) global symmetry

Lepton Flavours

e	μ	τ
ν_e	ν_μ	ν_τ

- Lepton Flavour Violation (LFV)
  - neutral LFV: ν_e, ν_μ, ν_τ
    $\rightarrow$ neutrino oscillations
  - charged LFV: e, μ, τ
    $\rightarrow$ only indirectly via ν_i

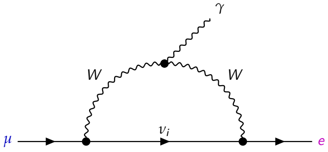

$\text{BR}(\mu \to e\gamma) \lesssim 10^{-50} \quad \left[\sim \left(\frac{\Delta m_\nu^2}{m_W^2} \right)^2 \right]$

Lepton Flavour Violation

- Search for new physics (NP):
  one prominent probe $\rightarrow$ LFV
- Lepton Flavour (LF) is conserved by SM
- LF is an (accidental) global symmetry

Lepton Flavours

e	μ	τ
ν_e	ν_μ	ν_τ

- Lepton Flavour Violation (LFV)
  - neutral LFV: ν_e, ν_μ, ν_τ
    $\rightarrow$ neutrino oscillations
  - charged LFV: e, μ, τ
    $\rightarrow$ only indirectly via ν_i

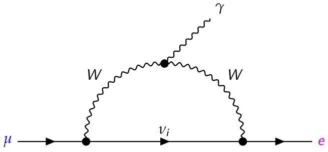

$\text{BR}(\mu \rightarrow e\gamma) \lesssim 10^{-50} \quad \left[\sim \left(\frac{\Delta m_\nu^2}{m_W^2}\right)^2\right]$

- Observation of CLFV would be NP

Very clean BSM signal (no competing SM)

LFV Experiments and current limits

LFV process	current limit	(planned) experiments
$\mu \to e\gamma$	$< 4.2 \cdot 10^{-13}$ [MEG]	MEG II
$\mu \to 3e$	$< 1.0 \cdot 10^{-12}$ [SINDRUM]	Mu3e
$\tau \to \ell\gamma, 3\ell, \ell P, \ldots$	$\lesssim 10^{-8}$ [Belle, LHCb, . . .]	Belle 2, . . .
$K \to \mu e, \mu e\pi, \mu e\pi\pi$	$\lesssim 10^{-11}$ [KTeV, NA62, BNL]	KOTO, LHCb

LFV Experiments and current limits

LFV process	current limit	(planned) experiments
$\mu \to e\gamma$	$< 4.2 \cdot 10^{-13}$ [MEG]	MEG II
$\mu \to 3e$	$< 1.0 \cdot 10^{-12}$ [SINDRUM]	Mu3e
$\tau \to \ell\gamma, 3\ell, \ell P, \ldots$	$\lesssim 10^{-8}$ [Belle, LHCb, ...]	Belle 2, ...
$K \to \mu e, \mu e\pi, \mu e\pi\pi$	$\lesssim 10^{-11}$ [KTeV, NA62, BNL]	KOTO, LHCb
$\pi^0 \to \bar{\mu}e$	$< 3.6 \cdot 10^{-10}$ [KTeV]	JEF, REDTOP
$\eta \to \bar{\mu}e$	$< 6 \cdot 10^{-6}$ [SPEC]	
$\eta' \to \bar{\mu}e$	$< 4.7 \cdot 10^{-4}$ [CLEO II]	

LFV Experiments and current limits

LFV process	current limit	(planned) experiments
$\mu \to e\gamma$	$< 4.2 \cdot 10^{-13}$ [MEG]	MEG II
$\mu \to 3e$	$< 1.0 \cdot 10^{-12}$ [SINDRUM]	Mu3e
$\tau \to \ell\gamma, 3\ell, \ell P, \ldots$	$\lesssim 10^{-8}$ [Belle, LHCb, . . .]	Belle 2, . . .
$K \to \mu e, \mu e\pi, \mu e\pi\pi$	$\lesssim 10^{-11}$ [KTeV, NA62, BNL]	KOTO, LHCb
$\pi^0 \to \bar{\mu}e$	$< 3.6 \cdot 10^{-10}$ [KTeV]	
$\eta \to \bar{\mu}e$	$< 6 \cdot 10^{-6}$ [SPEC]	JEF, REDTOP
$\eta' \to \bar{\mu}e$	$< 4.7 \cdot 10^{-4}$ [CLEO II]	
Au $\mu^- \to$ Au e^-	$< 7 \cdot 10^{-13}$ [SINDRUM II]	
Ti $\mu^- \to$ Ti e^-	$< 6.1 \cdot 10^{-13}$ [SINDRUM II]	
Al $\mu^- \to$ Al e^-	$\lesssim 10^{-17}$ (projected)	Mu2e, COMET

Major experimental improvements expected [see: LFV session this morning]

$\to$ stringent bounds on LFV

What is $\mu \to e$ conversion? (theorist's perspective)

- Experimental Setup:

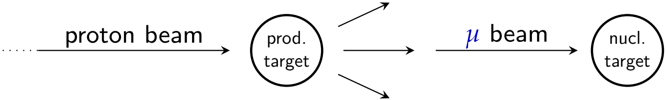

What is $\mu \to e$ conversion? (theorist's perspective)

- Experimental Setup:

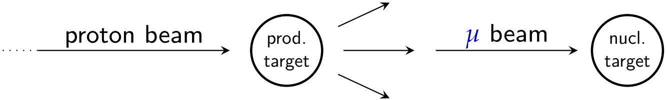

- Conversion process:
(within Coulomb field of the nucleus)

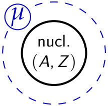

What is $\mu \to e$ conversion? (theorist's perspective)

- Experimental Setup:

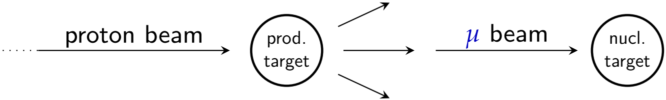

- Conversion process:
  (within Coulomb field of the nucleus)

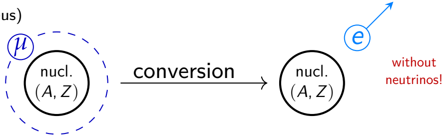

What is $\mu \to e$ conversion? (theorist's perspective)

- Experimental Setup:

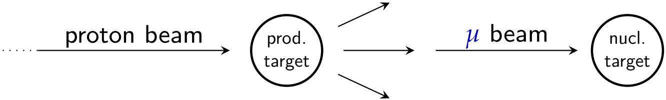

- Conversion process:
  (within Coulomb field of the nucleus)

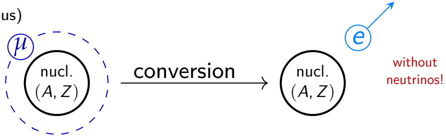

- Experimental signature:
  e^- with $q \approx m_\mu$
- Only background: decay in orbit
  $\mu^- \to \nu_\mu \bar{\nu}_e e^-$
- Normalisation: muon capture
  $\mu\,(A, Z) \to \nu_\mu\,(A, Z-1)$

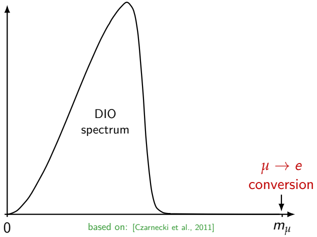

How to describe LFV from the theory side?

Standard Model EFT:

- Model-independent effective field theory description of BSM physics with higher dimensional operators obeying SM gauge symmetries:

$$\mathcal{L}^{\text{SM EFT}} = \mathcal{L}^{\text{SM}} + \frac{1}{\Lambda}\mathcal{L}^{(5)} + \frac{1}{\Lambda^2}\mathcal{L}^{(6)} + \dots$$

- Can be seen as the low-energy effective theory of any theory introducing new physics at high energies

How to describe LFV from the theory side?

Standard Model EFT:

- Model-independent effective field theory description of BSM physics with higher dimensional operators obeying SM gauge symmetries:

$$\mathcal{L}^{\text{SM EFT}} = \mathcal{L}^{\text{SM}} + \frac{1}{\Lambda}\mathcal{L}^{(5)} + \frac{1}{\Lambda^2}\mathcal{L}^{(6)} + \ldots$$

- Can be seen as the low-energy effective theory of any theory introducing new physics at high energies
- Naturally contains LFV operators:

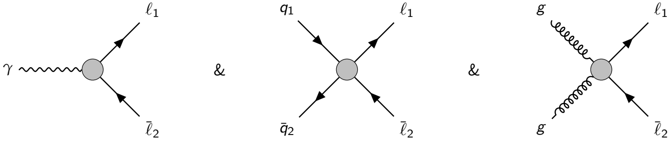

How to describe LFV from the theory side?

Standard Model EFT:

- Model-independent effective field theory description of BSM physics with higher dimensional operators obeying SM gauge symmetries:

$$\mathcal{L}^{\text{SM EFT}} = \mathcal{L}^{\text{SM}} + \frac{1}{\Lambda}\mathcal{L}^{(5)} + \frac{1}{\Lambda^2}\mathcal{L}^{(6)} + \dots$$

- Can be seen as the low-energy effective theory of any theory introducing new physics at high energies
- Naturally contains LFV operators:

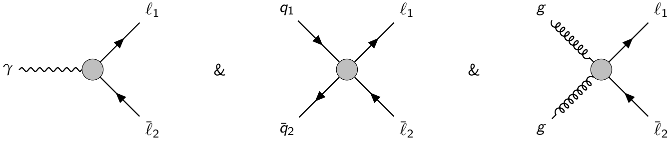

Can be used to describe all LFV processes in a model-independent way

How to use this for $\mu \to e$ conversion?

Many different scales matter:

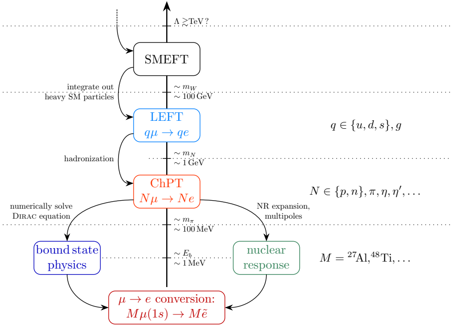

How to use this for $\mu \to e$ conversion?

Many different scales matter:

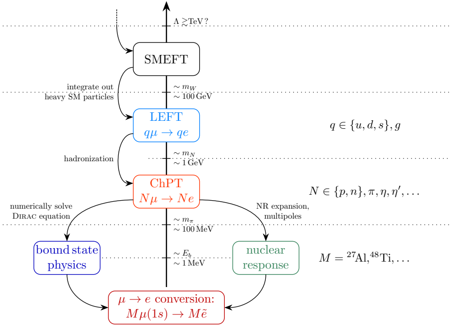

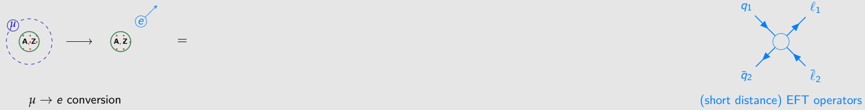

How to use this for $\mu \to e$ conversion?

Many different scales matter:

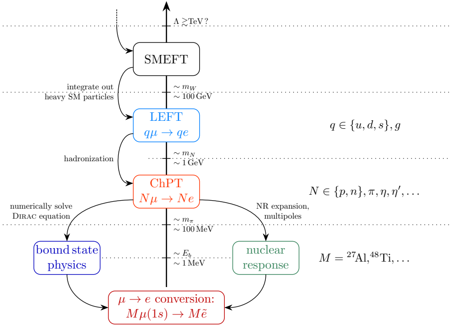

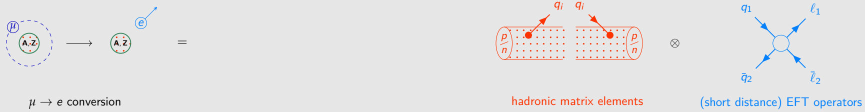

How to use this for $\mu \to e$ conversion?

Many different scales matter:

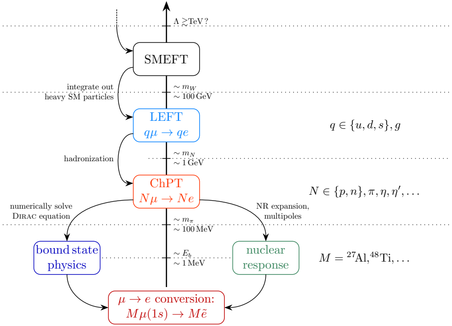

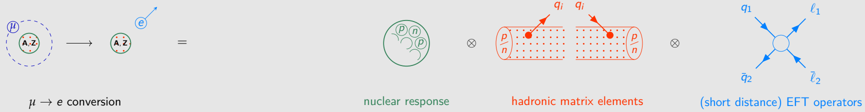

How to use this for $\mu \to e$ conversion?

Many different scales matter:

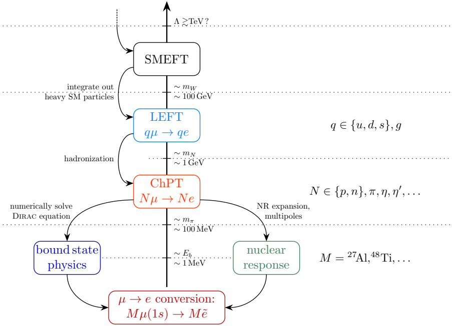

How to use this for $\mu \to e$ conversion?

Many different scales matter:

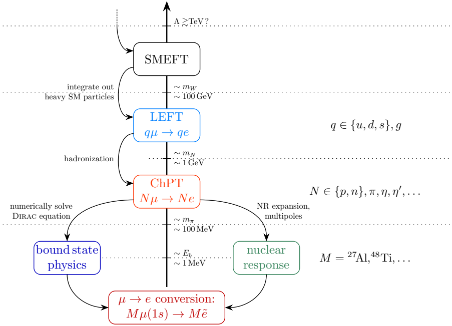

Objectives:

- Compare different probes:
  e.g.: $\mu \to e$ vs. $P \to \bar{\mu} e$
- Discriminate BSM operators

How to use this for $\mu \to e$ conversion?

Many different scales matter:

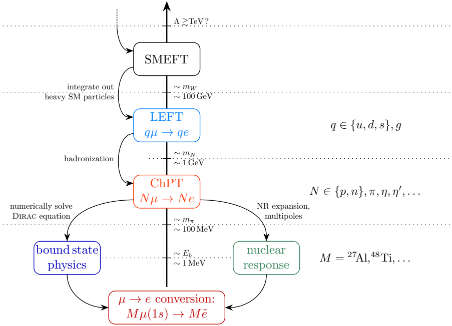

Objectives:

- Compare different probes: e.g.: $\mu \to e$ vs. $P \to \bar{\mu} e$
- Discriminate BSM operators
- Control theory uncertainties:
  - Hadronic matrix elements
  - Nuclear response
  - Coulomb corrections
- RG corrections

At all steps uncertainties need to be controlled!

Decomposition of the hadronic side

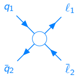

EFT operators

Decomposition of the hadronic side

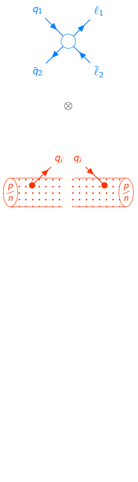

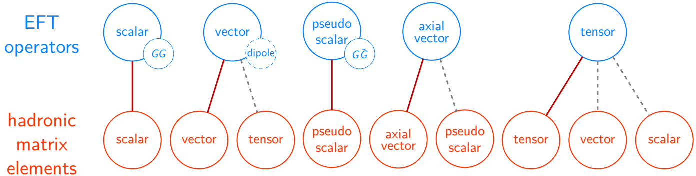

Decomposition of the hadronic side

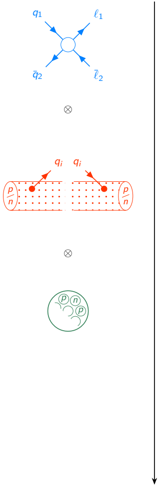

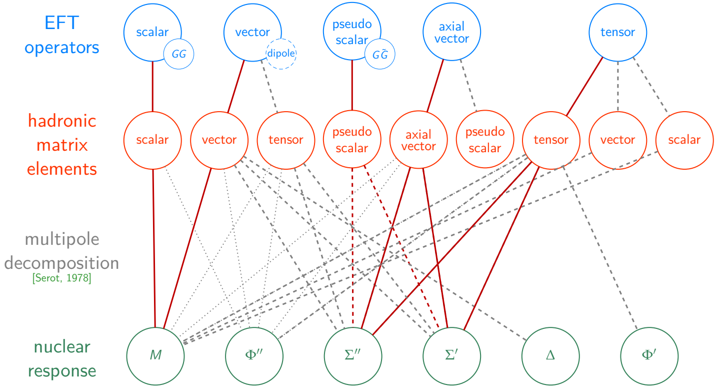

Decomposition of the hadronic side

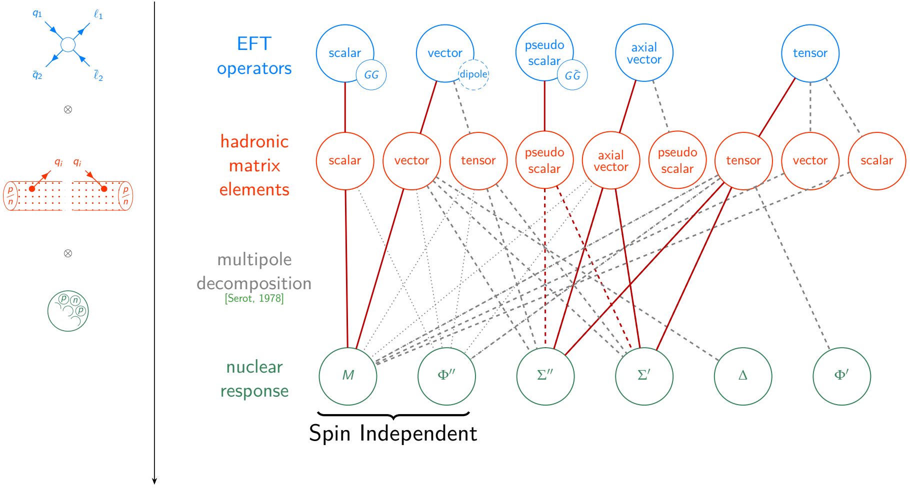

- SI: coherently enhanced; $\Gamma_{\text{SI}} \sim \# N^2$; e.g. [Kitano et al., 2002,...]

Decomposition of the hadronic side

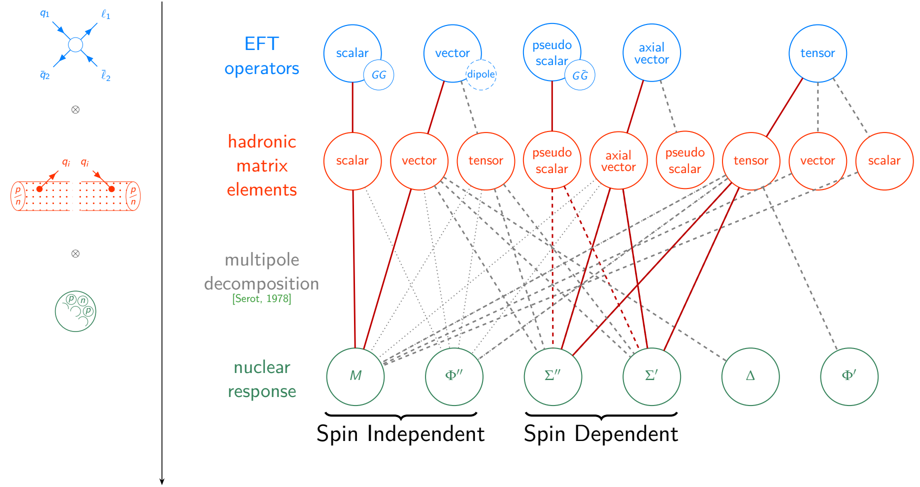

- SI: coherently enhanced; $\Gamma_{\text{SI}} \sim \# N^2$; e.g. [Kitano et al., 2002,. . .]
- SD: not coherently enhanced; only for $J > 0$; e.g. [Davidson et al., 2018,. . .]

Decomposition of the hadronic side

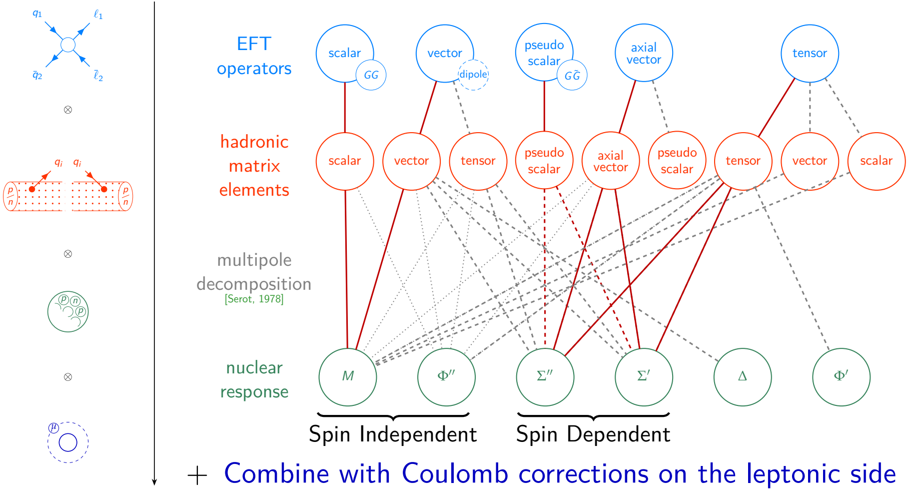

\+ Combine with Coulomb corrections on the leptonic side

- SI: coherently enhanced; $\Gamma_{SI} \sim \#N^2$; e.g. [Kitano et al., 2002,...]
- SD: not coherently enhanced; only for $J > 0$; e.g. [Davidson et al., 2018,...]

Deduced Limits for $P \to \mu e$

- Same underlying operators: P, A, $G\tilde{G}$, but not the same linear combinations

Deduced Limits for $P \to \mu e$

- Same underlying operators: $P, A, G\tilde{G}$,
  but not the same linear combinations
- Consider first one operator at a time:

$\mu \to e$ (exp.)	$P \to \bar{\mu} e$ (derived)	current limit
$\mathrm{BR}_{\mathrm{Ti}} < 6.1 \times 10^{-13}$	$\mathrm{BR}_{\pi^0} \lesssim 4 \times 10^{-17}$	$< 3.6 \times 10^{-10}$
	$\mathrm{BR}_{\eta} \lesssim 5 \times 10^{-13}$	$< 6.0 \times 10^{-6}$
	$\mathrm{BR}_{\eta'} \lesssim 7 \times 10^{-14}$	$< 4.7 \times 10^{-4}$

(scan over all "one operator at a time"-scenarios and choices for matrix elements)

Deduced Limits for $P \to \mu e$

- Same underlying operators: $P, A, G\tilde{G}$,
  but not the same linear combinations
- Consider first one operator at a time:

$\mu \to e$ (exp.)	$P \to \bar{\mu} e$ (derived)	current limit
$\mathrm{BR}_{\mathrm{Ti}} < 6.1 \times 10^{-13}$	$\mathrm{BR}_{\pi^0} \lesssim 4 \times 10^{-17}$	$< 3.6 \times 10^{-10}$
	$\mathrm{BR}_{\eta} \lesssim 5 \times 10^{-13}$	$< 6.0 \times 10^{-6}$
	$\mathrm{BR}_{\eta'} \lesssim 7 \times 10^{-14}$	$< 4.7 \times 10^{-4}$

(scan over all "one operator at a time"-scenarios and choices for matrix elements)

- For a rigorous limits we need to scan over all Wilson coefficients
  $\to \exists$ (fine-tuned) scenarios where $\mu \to e$ vanishes exactly
- In this scenario $\pi^0 \to \bar{\mu} e$ vanishes as well:

  rigorous limit: $\mathrm{Br}_{\pi^0 \to \bar{\mu} e} < 1.0 \times 10^{-13}$ $\quad$ $\left(\text{exp: } < 3.6 \cdot 10^{-10}\right)$

Deduced Limits for $P \to \mu e$

- Same underlying operators: $P, A, G\tilde{G}$,
  but not the same linear combinations
- Consider first one operator at a time:

$\mu \to e$ (exp.)	$P \to \bar{\mu}e$ (derived)	current limit
$\text{BR}_{\text{Ti}} < 6.1 \times 10^{-13}$	$\text{BR}_{\pi^0} \lesssim 4 \times 10^{-17}$	$< 3.6 \times 10^{-10}$
	$\text{BR}_{\eta} \lesssim 5 \times 10^{-13}$	$< 6.0 \times 10^{-6}$
	$\text{BR}_{\eta'} \lesssim 7 \times 10^{-14}$	$< 4.7 \times 10^{-4}$

(scan over all "one operator at a time"-scenarios and choices for matrix elements)

- For a rigorous limits we need to scan over all Wilson coefficients
  $\to \exists$ (fine-tuned) scenarios where $\mu \to e$ vanishes exactly
- In this scenario $\pi^0 \to \bar{\mu}e$ vanishes as well:
  rigorous limit: $\text{Br}_{\pi^0 \to \bar{\mu}e} < 1.0 \times 10^{-13}$ $\left(\text{exp: } < 3.6 \cdot 10^{-10}\right)$
- For $\eta^{(\prime)} \to \bar{\mu}e$: in principle, no strict limits
- Cancellation easily lifted by RG corrections
  [Crivellin et al., 2017; Cirigliano et al., 2017]

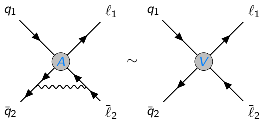

Future projection for $\pi^0 \to \bar{\mu}e$

With values from Mu2e or COMET the limits become even stronger

Future projection for $\pi^0 \to \bar{\mu} e$

With values from Mu2e or COMET the limits become even stronger

- Combining the limits from Ti and Al we find:

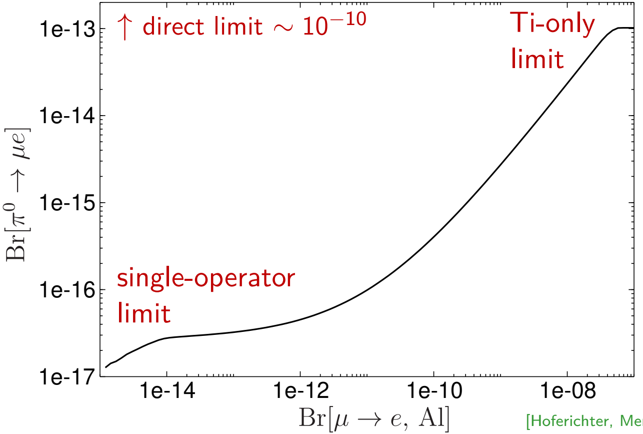

[Hoferichter, Menéndez, FN, 2023]

Controlling uncertainties

- Hadronic matrix elements: from LatticeQCD & Phenomenology

Controlling uncertainties

- Hadronic matrix elements: from LatticeQCD & Phenomenology
- Nuclear structure:
  - So far: (empirical) nuclear shell-model calculations:
    $\rightarrow$ Uncertainty estimate difficult; esp. for neutron response

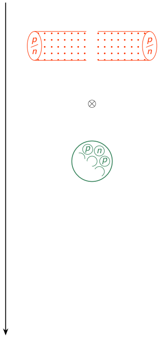

Controlling uncertainties

- Hadronic matrix elements: from LatticeQCD & Phenomenology
- Nuclear structure:
  - So far: (empirical) nuclear shell-model calculations:
    → Uncertainty estimate difficult; esp. for neutron response
  - Ab-initio approaches:
    → Often uncertainties dominated by chiral Hamiltonian and not by many-body solutions
    → Often correlations between responses much more stable

[Hagen et al., 2016; Payne et al., 2019]

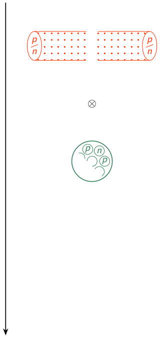

Controlling uncertainties

- Hadronic matrix elements: from LatticeQCD & Phenomenology
- Nuclear structure:
  - So far: (empirical) nuclear shell-model calculations:
    $\rightarrow$ Uncertainty estimate difficult; esp. for neutron response
  - Ab-initio approaches:
    $\rightarrow$ Often uncertainties dominated by chiral Hamiltonian and not by many-body solutions
    $\rightarrow$ Often correlations between responses much more stable
    [Hagen et al., 2016; Payne et al., 2019]
  - Charge form factor given by charge density mediates dipole and overlaps with M, Φ'' response

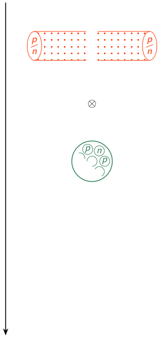

Controlling uncertainties

- Hadronic matrix elements: from LatticeQCD & Phenomenology
- Nuclear structure:
  - So far: (empirical) nuclear shell-model calculations:
    $\rightarrow$ Uncertainty estimate difficult; esp. for neutron response
  - Ab-initio approaches:
    $\rightarrow$ Often uncertainties dominated by chiral Hamiltonian and not by many-body solutions
    $\rightarrow$ Often correlations between responses much more stable
    [Hagen et al., 2016; Payne et al., 2019]
  - Charge form factor given by charge density mediates dipole and overlaps with M, Φ'' response
- Bound-state physics:
  - Solve Dirac eq. in nucleus potential given by charge density

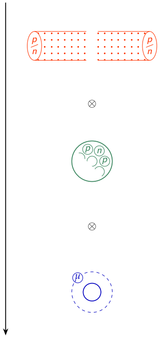

Controlling uncertainties

- Hadronic matrix elements: from LatticeQCD & Phenomenology
- Nuclear structure:
  - So far: (empirical) nuclear shell-model calculations:
    → Uncertainty estimate difficult; esp. for neutron response
  - Ab-initio approaches:
    → Often uncertainties dominated by chiral Hamiltonian and not by many-body solutions
    → Often correlations between responses much more stable
    [Hagen et al., 2016; Payne et al., 2019]
  - Charge form factor given by charge density mediates dipole and overlaps with M, Φ'' response
- Bound-state physics:
  - Solve Dirac eq. in nucleus potential given by charge density

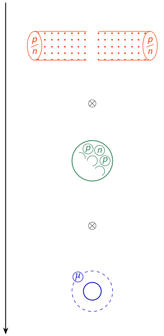

Charge densities with quantified uncertainties required

Controlling uncertainties

- Hadronic matrix elements: from LatticeQCD & Phenomenology
- Nuclear structure:
  - So far: (empirical) nuclear shell-model calculations:
    $\rightarrow$ Uncertainty estimate difficult; esp. for neutron response
  - Ab-initio approaches:
    $\rightarrow$ Often uncertainties dominated by chiral Hamiltonian and not by many-body solutions
    $\rightarrow$ Often correlations between responses much more stable
    [Hagen et al., 2016; Payne et al., 2019]
  - Charge form factor given by charge density mediates dipole and overlaps with M, Φ'' response
- Bound-state physics:
  - Solve Dirac eq. in nucleus potential given by charge density

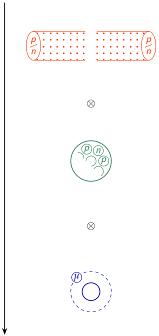

Charge densities with quantified uncertainties required

So far: As Fourier-Bessel series without uncertainties [Vries et al., 1987]
$\rightarrow$ Redo extraction from elastic electron nucleus scattering

Electron scattering and Coulomb corrections

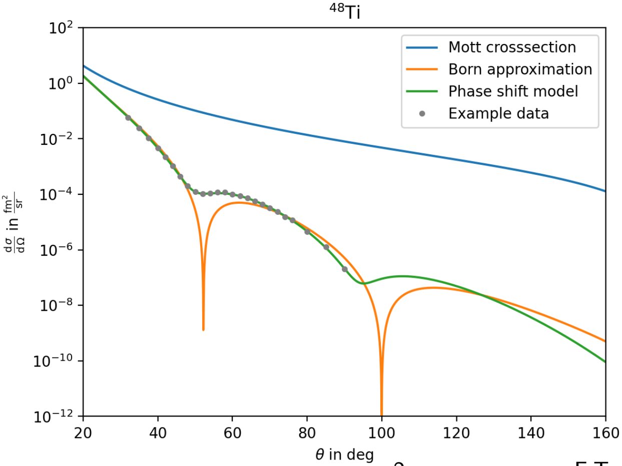

- With plane waves ($J = 0$): $\frac{d\sigma}{d\Omega} \sim \left| F_0^{ch} \right|^2$; $\quad F_0^{ch}(q) \overset{\text{F.T.}}{\longleftrightarrow} \rho_0(r)$
- Coulomb corrections fill out minima and shift the crosssection
  $\rightarrow$ Included by numerically solving Dirac equation

Extracting charge densities from electron scattering

- Fourier-Bessel parameterization:
  ($q_n = \frac{n\pi}{R}$ s.t. $j_0(q_n R) = 0$) [Dreher et al., 1974]

$$\rho_0(r) = \begin{cases} \sum_{n=1}^{N} a_n \, j_0(q_n r) & , \; r \leq R \\ 0 & , \; r > R \end{cases}$$

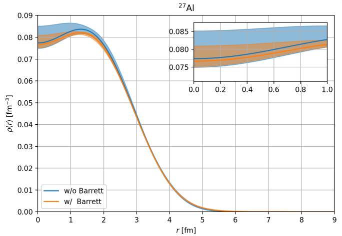

[FN, Hoferichter, 2024]

Extracting charge densities from electron scattering

- Fourier-Bessel parameterization:
  ($q_n = \frac{n\pi}{R}$ s.t. $j_0(q_n R) = 0$) [Dreher et al., 1974]

$$\rho_0(r) = \begin{cases} \sum_{n=1}^{N} a_n \, j_0(q_n r) & , \; r \leq R \\ 0 & , \; r > R \end{cases}$$

- Practical challenges:
  - Most data from the 70s & 80s
  - Many datasets not available at all or only in PhD theses
  - Uncertainty documentation rudimentary
  - Computationally intensive (w.r.t. uncertainties)

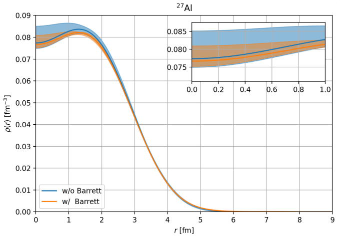

[FN, Hoferichter, 2024]

Extracting charge densities from electron scattering

- Fourier-Bessel parameterization:
  ($q_n = \frac{n\pi}{R}$ s.t. $j_0(q_n R) = 0$) [Dreher et al., 1974]

$$\rho_0(r) = \begin{cases} \sum_{n=1}^{N} a_n\, j_0(q_n r) & , \; r \leq R \\ 0 & , \; r > R \end{cases}$$

- Practical challenges:
  - Most data from the 70s & 80s
  - Many datasets not available at all or only in PhD theses
  - Uncertainty documentation rudimentary
  - Computationally intensive (w.r.t. uncertainties)
- Scan over R, N → estimate systematics
- Constraints from muonic atoms (Barrett moment)
- Suppress overparametrization (asymptotics)

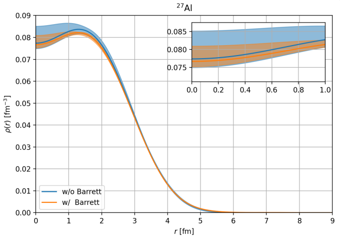

[FN, Hoferichter, 2024]

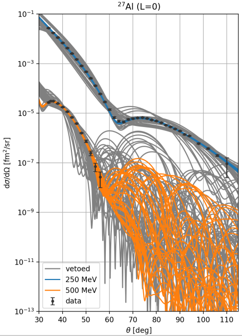

Extracting charge densities from electron scattering

- Fourier-Bessel parameterization:
  ($q_n = \frac{n\pi}{R}$ s.t. $j_0(q_n R) = 0$) [Dreher et al., 1974]

$$\rho_0(r) = \begin{cases} \sum_{n=1}^{N} a_n\, j_0(q_n r) & , \; r \leq R \\ 0 & , \; r > R \end{cases}$$

- Practical challenges:
  - Most data from the 70s & 80s
  - Many datasets not available at all or only in PhD theses
  - Uncertainty documentation rudimentary
  - Computationally intensive (w.r.t. uncertainties)
- Scan over R, N → estimate systematics
- Constraints from muonic atoms (Barrett moment)
- Suppress overparametrization (asymptotics)

Carried out for ^{27}Al, ^{40,48}Ca, ^{48,50}Ti

Results available in python notebook [2406.06677]

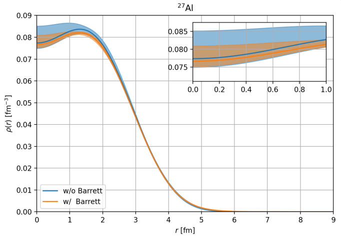

[FN, Hoferichter, 2024]

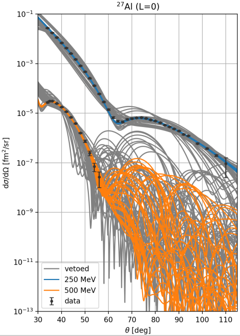

SI $\mu \to e$ conversion

- Coherently enhanced multipoles: Scalar, Vector and Dipole interactions

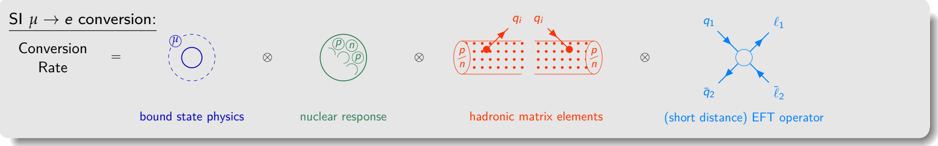

SI $\mu \to e$ conversion

- Coherently enhanced multipoles: Scalar, Vector and Dipole interactions

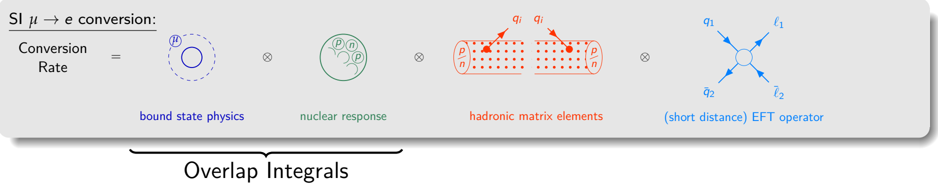

SI $\mu \to e$ conversion

- Coherently enhanced multipoles: Scalar, Vector and Dipole interactions

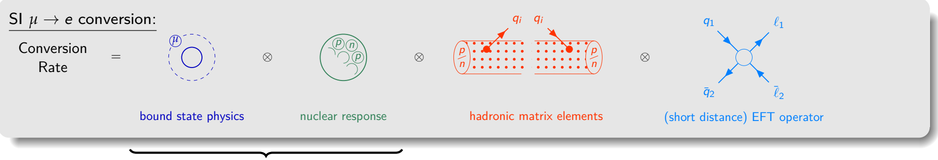

[Kitano et al., 2002]

$$S^{(N)} = \frac{1}{2\sqrt{2}} \int_0^\infty \mathrm{d}r \, (\#N)\rho_N(r) \left[g_{-1}^{(e)}(r) g_{-1}^{(\mu)}(r) - f_{-1}^{(e)}(r) f_{-1}^{(\mu)}(r) \right]$$

$$V^{(N)} = \frac{1}{2\sqrt{2}} \int_0^\infty \mathrm{d}r \, (\#N)\rho_N(r) \left[g_{-1}^{(e)}(r) g_{-1}^{(\mu)}(r) + f_{-1}^{(e)}(r) f_{-1}^{(\mu)}(r) \right]$$

$$D = -\frac{4}{\sqrt{2}} m_\mu \int_0^\infty \mathrm{d}r \, E(r) \underbrace{\left[g_{-1}^{(e)}(r) \, f_{-1}^{(\mu)}(r) + f_{-1}^{(e)}(r) \, g_{-1}^{(\mu)}(r) \right]}_{\text{electron and muon wave functions}}$$

SI $\mu \to e$ conversion

- Coherently enhanced multipoles: Scalar, Vector and Dipole interactions

SI $\mu \to e$ conversion:

Conversion Rate =

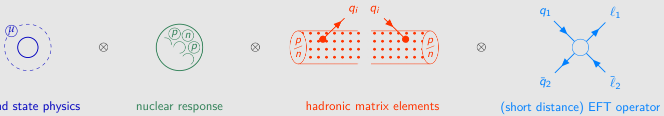

Overlap Integrals

[Kitano et al., 2002]

$$S^{(N)} = \frac{1}{2\sqrt{2}} \int_0^\infty \mathrm{d}r \, (\#N)\rho_N(r) \left[g_{-1}^{(e)}(r) g_{-1}^{(\mu)}(r) - f_{-1}^{(e)}(r) f_{-1}^{(\mu)}(r) \right]$$

$$V^{(N)} = \frac{1}{2\sqrt{2}} \int_0^\infty \mathrm{d}r \, (\#N)\rho_N(r) \left[g_{-1}^{(e)}(r) g_{-1}^{(\mu)}(r) + f_{-1}^{(e)}(r) f_{-1}^{(\mu)}(r) \right]$$

$$D = -\frac{4}{\sqrt{2}} m_\mu \int_0^\infty \mathrm{d}r \, E(r) \underbrace{\left[g_{-1}^{(e)}(r) \, f_{-1}^{(\mu)}(r) + f_{-1}^{(e)}(r) \, g_{-1}^{(\mu)}(r) \right]}_{\text{electron and muon wave functions}}$$

Employ extracted charge densities with uncertainties

Overlap integrals

Dipole: $$D = -\frac{4}{\sqrt{2}} m_\mu \int_0^\infty \mathrm{d}r \, E(r) \left[g_{-1}^{(e)}(r) \, f_{-1}^{(\mu)}(r) + f_{-1}^{(e)}(r) \, g_{-1}^{(\mu)}(r) \right]$$

Overlap integrals

Dipole: $D = -\frac{4}{\sqrt{2}} m_\mu \int_0^\infty \mathrm{d}r\, E(r) \left[g_{-1}^{(e)}(r)\, f_{-1}^{(\mu)}(r) + f_{-1}^{(e)}(r)\, g_{-1}^{(\mu)}(r) \right]$

- Only depends on charge density ρ_0 (electric field $E(r) \leftarrow \rho_0(r)$)

Overlap integrals

Dipole: $D = -\frac{4}{\sqrt{2}} m_\mu \int_0^\infty \mathrm{d}r\, E(r) \left[g_{-1}^{(e)}(r)\, f_{-1}^{(\mu)}(r) + f_{-1}^{(e)}(r)\, g_{-1}^{(\mu)}(r) \right]$

- Only depends on charge density ρ_0 (electric field $E(r) \leftarrow \rho_0(r)$)

$D(^{40}\mathrm{Ca}) = 0.07531(5)$ $\qquad$ $D(^{48}\mathrm{Ca}) = 0.07479(10)$

$D(^{48}\mathrm{Ti}) = 0.0864(1)$ $\qquad$ $D(^{27}\mathrm{Al}) = 0.0359(2)$

- For the first time: Fully quantified uncertainties

Overlap integrals

Dipole: $D = -\frac{4}{\sqrt{2}} m_\mu \int_0^\infty \mathrm{d}r\, E(r) \left[g_{-1}^{(e)}(r)\, f_{-1}^{(\mu)}(r) + f_{-1}^{(e)}(r)\, g_{-1}^{(\mu)}(r) \right]$

- Only depends on charge density ρ_0 (electric field $E(r) \leftarrow \rho_0(r)$)

$D(^{40}\mathrm{Ca}) = 0.07531(5)$ $\quad$ $D(^{48}\mathrm{Ca}) = 0.07479(10)$

$D(^{48}\mathrm{Ti}) = 0.0864(1)$ $\quad$ $D(^{27}\mathrm{Al}) = 0.0359(2)$

- For the first time: Fully quantified uncertainties

Scalar & Vector: $S^{(N)}, V^{(N)} \supset \rho_N \longleftrightarrow M_N$ response

Overlap integrals

Dipole: $$D = -\frac{4}{\sqrt{2}} m_\mu \int_0^\infty \mathrm{d}r\, E(r) \left[g_{-1}^{(e)}(r)\, f_{-1}^{(\mu)}(r) + f_{-1}^{(e)}(r)\, g_{-1}^{(\mu)}(r) \right]$$

- Only depends on charge density ρ_0 (electric field $E(r) \leftarrow \rho_0(r)$)

$$D(^{40}\mathrm{Ca}) = 0.07531(5) \qquad D(^{48}\mathrm{Ca}) = 0.07479(10)$$
$$D(^{48}\mathrm{Ti}) = 0.0864(1) \qquad D(^{27}\mathrm{Al}) = 0.0359(2)$$

- For the first time: Fully quantified uncertainties

Scalar & Vector: $S^{(N)}, V^{(N)} \supset \rho_N \longleftrightarrow M_N$ response

- Requires proton and neutron densities:
  - $\rho_p \approx \rho_0$ (from electron scattering)
  - $\rho_n \approx \rho_\mathrm{w}$ (from parity violating electron scattering)

  $\rightarrow$ Not ideal, PVES only recently measured and only for a few nuclei

Overlap integrals

Dipole: $D = -\frac{4}{\sqrt{2}} m_\mu \int_0^\infty \mathrm{d}r\, E(r) \left[g_{-1}^{(e)}(r)\, f_{-1}^{(\mu)}(r) + f_{-1}^{(e)}(r)\, g_{-1}^{(\mu)}(r) \right]$

- Only depends on charge density ρ_0 (electric field $E(r) \leftarrow \rho_0(r)$)

$$D(^{40}\mathrm{Ca}) = 0.07531(5) \qquad D(^{48}\mathrm{Ca}) = 0.07479(10)$$
$$D(^{48}\mathrm{Ti}) = 0.0864(1) \qquad D(^{27}\mathrm{Al}) = 0.0359(2)$$

- For the first time: Fully quantified uncertainties

Scalar & Vector: $S^{(N)}, V^{(N)} \supset \rho_N \longleftrightarrow M_N$ response

- Requires proton and neutron densities:
  - $\rho_p \approx \rho_0$ (from electron scattering)
  - $\rho_n \approx \rho_w$ (from parity violating electron scattering)

  $\rightarrow$ Not ideal, PVES only recently measured and only for a few nuclei

Alternative: Correlate using ab-initio methods

Correlations

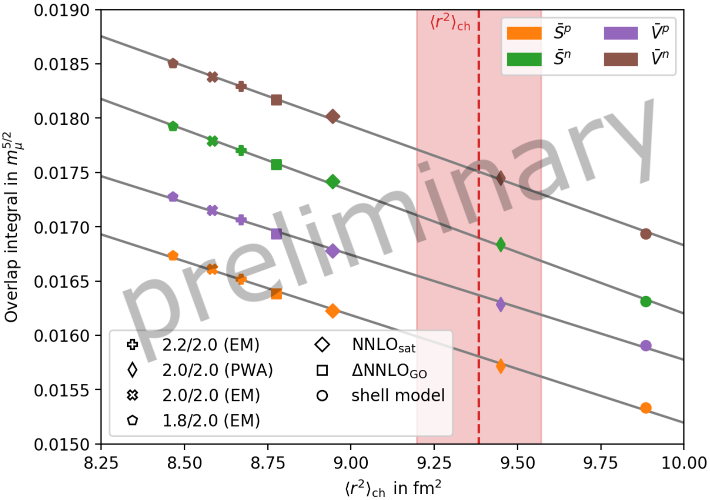

[Heinz, Hoferichter, Miyagi, FN, Schwenk, in preparation]

- Calculated using IMSRG for ^{27}Al

Conclusion

Summary:

- LFV is a promising BSM probe
  with lots of experimental developments
- EFT for $\mu \to e$ conversion in nuclei
  - Discriminate LFV mechanisms
  - Controlled uncertainty estimates

Conclusion

Summary:

- LFV is a promising BSM probe
  with lots of experimental developments
- EFT for $\mu \to e$ conversion in nuclei
  - Discriminate LFV mechanisms
  - Controlled uncertainty estimates

Recent results:

- Indirect limits for $P \to \bar{\mu} e$
- Uncertainty estimates for charge densities
  and their propagation

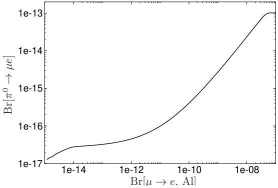

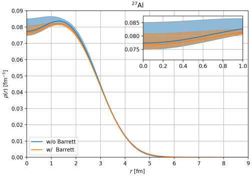

Conclusion

Summary:

- LFV is a promising BSM probe
  with lots of experimental developments
- EFT for $\mu \to e$ conversion in nuclei
  - Discriminate LFV mechanisms
  - Controlled uncertainty estimates

Recent results:

- Indirect limits for $P \to \bar{\mu}e$
- Uncertainty estimates for charge densities
  and their propagation

Outlook:

- Overlap integrals from ab-initio calculations
- Phase-shift model `python` package
- Subleading nuclear responses; two-body currents

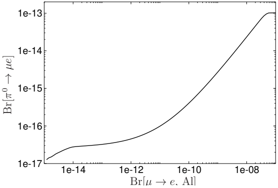

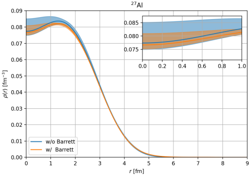

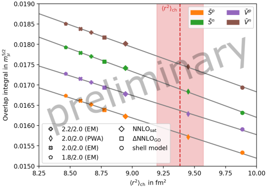

Thank you for your attention!

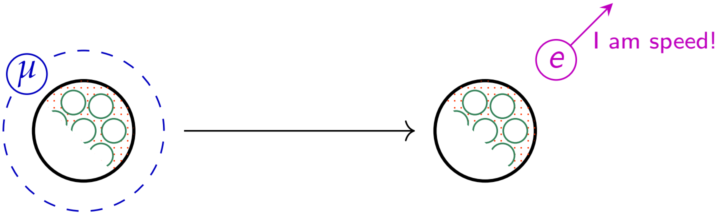

References I

Hoferichter, M., J. Menéndez, and F. Noël (Apr. 2023). "Improved Limits on Lepton-Flavor-Violating Decays of Light Pseudoscalars via Spin-Dependent $\mu \to e$ Conversion in Nuclei". In: *Phys. Rev. Lett.* 130.13, p. 131902. DOI: 10.1103/PhysRevLett.130.131902. arXiv: 2204.06005 [hep-ph].

Noël, F. and M. Hoferichter (2024). "Uncertainty quantification for $\mu \to e$ conversion in nuclei: charge distributions". In: *JHEP* 08, p. 052. DOI: 10.1007/JHEP08(2024)052. arXiv: 2406.06677 [nucl-th].

Heinz, M. et al. (2024). in preparation.

Baldini, A. M. et al. (2016). "Search for the lepton flavour violating decay $\mu^+ \to \mathrm{e}^+\gamma$ with the full dataset of the MEG experiment". In: *Eur. Phys. J. C* 76.8, p. 434. DOI: 10.1140/epjc/s10052-016-4271-x. arXiv: 1605.05081 [hep-ex].

Bellgardt, U. et al. (1988). "Search for the Decay $\mu^+ \to e^+e^+e^-$". In: *Nucl. Phys. B* 299, pp. 1–6. DOI: 10.1016/0550-3213(88)90462-2.

Wintz, P. (1998). "Results of the SINDRUM-II experiment". In: *Conf. Proc. C* 980420. Ed. by H. V. Klapdor-Kleingrothaus and I. V. Krivosheina, pp. 534–546.

Bertl, W. H. et al. (2006). "A Search for muon to electron conversion in muonic gold". In: *Eur. Phys. J. C* 47, pp. 337–346. DOI: 10.1140/epjc/s2006-02582-x.

Baldini, A. M. et al. (2018). "The design of the MEG II experiment". In: *Eur. Phys. J. C* 78.5, p. 380. DOI: 10.1140/epjc/s10052-018-5845-6. arXiv: 1801.04688 [physics.ins-det].

Arndt, K. et al. (2021). "Technical design of the phase I Mu3e experiment". In: *Nucl. Instrum. Meth. A* 1014, p. 165679. DOI: 10.1016/j.nima.2021.165679. arXiv: 2009.11690 [physics.ins-det].

Aiba, M. et al. (Nov. 2021). "Science Case for the new High-Intensity Muon Beams HIMB at PSI". In: DOI: 10.48550/arxiv.2111.05788. arXiv: 2111.05788 [hep-ex].

Bartoszek, L. et al. (Oct. 2014). "Mu2e Technical Design Report". In: DOI: 10.2172/1172555. arXiv: 1501.05241 [physics.ins-det].

Abramishvili, R. et al. (2020). "COMET Phase-I Technical Design Report". In: *PTEP* 2020.3, p. 033C01. DOI: 10.1093/ptep/ptz125. arXiv: 1812.09018 [physics.ins-det].

Appel, R. et al. (2000). "An Improved limit on the rate of decay $K^+ \to \pi^+\mu^+e^-$". In: *Phys. Rev. Lett.* 85, pp. 2450–2453. DOI: 10.1103/PhysRevLett.85.2450. arXiv: hep-ex/0005016.

Cortina Gil, E. et al. (2021). "Search for Lepton Number and Flavor Violation in K^+ and π^0 Decays". In: *Phys. Rev. Lett.* 127.13, p. 131802. DOI: 10.1103/PhysRevLett.127.131802. arXiv: 2105.06759 [hep-ex].

References II

Abouzaid, E. et al. (2008). “Search for lepton flavor violating decays of the neutral kaon”. In: *Phys. Rev. Lett.* 100, p. 131803. DOI: 10.1103/PhysRevLett.100.131803. arXiv: 0711.3472 [hep-ex].

White, D. B. et al. (1996). “Search for the decays $\eta \to \mu e$ and $\eta \to e^+e^-$”. In: *Phys. Rev. D* 53, pp. 6658–6661. DOI: 10.1103/PhysRevD.53.6658.

Briere, R. A. et al. (2000). “Rare decays of the η'”. In: *Phys. Rev. Lett.* 84, pp. 26–30. DOI: 10.1103/PhysRevLett.84.26. arXiv: hep-ex/9907046.

Gan, L. et al. (n.d.). *Eta Decays with Emphasis on Rare Neutral Modes: The JLab Eta Factory (JEF) Experiment, JLab proposal.* https://www.jlab.org/exp_prog/proposals/14/PR12-14-004.pdf.

Elam, J. et al. (Mar. 2022). “The REDTOP experiment: Rare η/η' Decays To Probe New Physics”. In: DOI: 10.48550/arxiv.2203.07651. arXiv: 2203.07651 [hep-ex].

Anzivino, G. et al. (2024). “Workshop summary: Kaons@CERN 2023”. In: *Eur. Phys. J. C* 84.4, p. 377. DOI: 10.1140/epjc/s10052-024-12565-4. arXiv: 2311.02923 [hep-ph].

Aoki, K. et al. (Oct. 2021). “Extension of the J-PARC Hadron Experimental Facility: Third White Paper”. In: arXiv: 2110.04462 [nucl-ex].

Ambrose, D. et al. (1998). “New limit on muon and electron lepton number violation from $K^0_L \to \mu^\pm e^\mp$ decay”. In: *Phys. Rev. Lett.* 81, pp. 5734–5737. DOI: 10.1103/PhysRevLett.81.5734. arXiv: hep-ex/9811038.

Sher, A. et al. (2005). “An Improved upper limit on the decay $K^+ \to \pi^+\mu^+e^-$”. In: *Phys. Rev. D* 72, p. 012005. DOI: 10.1103/PhysRevD.72.012005. arXiv: hep-ex/0502020.

Czarnecki, A., X. Garcia i Tormo, and W. J. Marciano (2011). “Muon decay in orbit: spectrum of high-energy electrons”. In: *Phys. Rev. D* 84, p. 013006. DOI: 10.1103/PhysRevD.84.013006. arXiv: 1106.4756 [hep-ph].

Suzuki, T., D. F. Measday, and J. P. Roalsvig (1987). “Total Nuclear Capture Rates for Negative Muons”. In: *Phys. Rev. C* 35, p. 2212. DOI: 10.1103/PhysRevC.35.2212.

Kitano, R., M. Koike, and Y. Okada (2002). “Detailed calculation of lepton flavor violating muon electron conversion rate for various nuclei”. In: *Phys. Rev. D* 66. [Erratum: Phys. Rev. D **76**, 059902 (2007)], p. 096002. DOI: 10.1103/PhysRevD.76.059902. arXiv: hep-ph/0203110.

Davidson, S., Y. Kuno, and A. Saporta (2018). ““Spin-dependent” $\mu \to e$ conversion on light nuclei”. In: *Eur. Phys. J. C* 78.2, p. 109. DOI: 10.1140/epjc/s10052-018-5584-8. arXiv: 1710.06787 [hep-ph].

References III

Serot, B. D. (1978).
"Semileptonic Weak and Electromagnetic Interactions with Nuclei: Nuclear Current Operators Through Order $(v/c)^2_{\text{nucleon}}$".
In: *Nucl. Phys. A* 308, pp. 457–499. DOI: 10.1016/0375-9474(78)90561-4.

Crivellin, A. et al. (2017).
"Renormalisation-group improved analysis of $\mu \to e$ processes in a systematic effective-field-theory approach".
In: *JHEP* 05, p. 117. DOI: 10.1007/JHEP05(2017)117. arXiv: 1702.03020 [hep-ph].

Cirigliano, V., S. Davidson, and Y. Kuno (2017). "Spin-dependent $\mu \to e$ conversion". In: *Phys. Lett. B* 771, pp. 242–246. DOI: 10.1016/j.physletb.2017.05.053. arXiv: 1703.02057 [hep-ph].

Hagen, G. et al. (2016). "Neutron and weak-charge distributions of the ^{48}Ca nucleus". In: *Nature Phys.* 12.2, pp. 186–190. DOI: 10.1038/nphys3529. arXiv: 1509.07169 [nucl-th].

Payne, C. G. et al. (2019). "Coherent elastic neutrino-nucleus scattering on ^{40}Ar from first principles".
In: *Phys. Rev. C* 100.6, p. 061304. DOI: 10.1103/PhysRevC.100.061304. arXiv: 1908.09739 [nucl-th].

Vries, H. de, C. W. de Jager, and C. de Vries (1987).
"Nuclear charge and magnetization density distribution parameters from elastic electron scattering".
In: *Atom. Data Nucl. Data Tabl.* 36, pp. 495–536. DOI: 10.1016/0092-640X(87)90013-1.

Dreher, B. et al. (Dec. 1974).
"The determination of the nuclear ground state and transition charge density from measured electron scattering data".
In: *Nucl. Phys. A* 235.1, pp. 219–248. DOI: 10.1016/0375-9474(74)90189-4.

Gan, L. et al. (2022). "Precision tests of fundamental physics with η and η' mesons". In: *Phys. Rept.* 945, p. 2191. DOI: 10.1016/j.physrep.2021.11.001. arXiv: 2007.00664 [hep-ph].

Escribano, R. et al. (2016). "η' transition form factor from space- and timelike experimental data".
In: *Phys. Rev. D* 94.5, p. 054033. DOI: 10.1103/PhysRevD.94.054033. arXiv: 1512.07520 [hep-ph].

Bali, G. S. et al. (2021). "Masses and decay constants of the η and η' mesons from lattice QCD". In: *JHEP* 08, p. 137. DOI: 10.1007/JHEP08(2021)137. arXiv: 2106.05398 [hep-lat].

Hoferichter, M., J. Menéndez, and A. Schwenk (2020).
"Coherent elastic neutrino-nucleus scattering: EFT analysis and nuclear responses". In: *Phys. Rev. D* 102.7, p. 074018. DOI: 10.1103/PhysRevD.102.074018. arXiv: 2007.08529 [hep-ph].

References IV

Airapetian, A. et al. (2007). "Precise determination of the spin structure function g(1) of the proton, deuteron and neutron". In: *Phys. Rev. D* 75, p. 012007. DOI: 10.1103/PhysRevD.75.012007. arXiv: hep-ex/0609039.

Backup-Slides

Description of $\mu \to e$ conversion

Effective description by separation of the appearing scales

Conversion Rate =

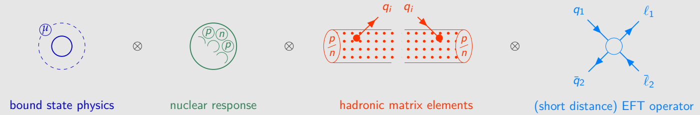

- EFT operators from Lagranian: $L^\Gamma \in \{\bar{e}_\Upsilon \mu, \bar{e}_\Upsilon \gamma_\mu \mu, \bar{e}_\Upsilon \sigma_{\mu\nu}\mu\}$, $(\Gamma = S, P, V, A, T, D, GG, G\tilde{G})$
  $\mathcal{L}_{\text{eff}} = \frac{1}{\Lambda^2}\sum_\Gamma \; C_q^\Gamma \; (L^\Gamma \cdot Q^{\Gamma,q})$ $\quad Q^{\Gamma,q} \in \left\{\bar{q}q, \bar{q}\gamma^5 q, \bar{q}\gamma^\mu q, \bar{q}\gamma^\mu\gamma^5 q, \bar{q}\sigma^{\mu\nu}q, F^{\mu\nu}, G^a_{\mu\nu}G^{\mu\nu}_a, G^a_{\mu\nu}\tilde{G}^{\mu\nu}_a\right\}$

- hadronic matrix elements:
  $\langle N| \, Q^{\Gamma,q} \, |N\rangle \to\sim F^{\Gamma,i}_{q,N} \; \bar{u}_N \mathcal{O}_i u_N \xrightarrow{\text{non.rel.}} \sim \bar{u}_N^{\text{NR}} \mathcal{O}_i^{\text{NR}} u_N^{\text{NR}}$

- nuclear multipoles (shell-model): $\quad \mathcal{O}_i^{\text{NR}} \in \left\{\mathbb{1}, \vec{\sigma}, \vec{\nabla}, \text{...and all combinations}\right\}$
  $\langle M| \, \mathcal{O}_i^{\text{NR}} \, |M\rangle \to\sim \mathcal{F}^{\mathcal{S}_N}$ $\quad \mathcal{S} \in \left\{M, \Sigma^{(\prime\prime)}, \Phi^{(\prime\prime)}, \Delta^{(\prime\prime)}, \Omega^{(\prime\prime)}, \Gamma^{(\prime\prime)}, \Pi^{(\prime\prime)}, \Theta^{(\prime\prime)}\right\}$

- bound state physics (numerical):
  $\langle \tilde{e}| \, L^\Gamma \, |\mu(1s)\rangle \to\sim \overline{\Psi_e}\mathcal{O}_\Gamma \Psi_\mu$ with $\Psi_e, \Psi_\mu \xleftarrow{\text{Dirac-eq.}} V(r) \leftarrow \rho_{\text{ch}}(r)$

Application: Indirect limits for $P \to \bar{\mu} e$ from $\mu \to e$

- Same operators probe SD $\mu \to e$ conversion and $P \to \bar{\mu} e$: [Gan et al., 2022]

$$\mathcal{L}_{\text{eff}} \supset \frac{1}{\Lambda^2} \sum_{\substack{Y=L,R \\ q=u,d,s}} \left[C_Y^{P,q} (\overline{e_Y} \mu)(\bar{q}\gamma_5 q) + C_Y^{A,q} (\overline{e_Y}\gamma^\mu \mu)(\bar{q}\gamma_\mu\gamma_5 q) \right] + \frac{i\alpha_s}{\Lambda^3} \sum_{Y=L,R} C_Y^{G\tilde{G}} (\overline{e_Y}\mu) G^a_{\mu\nu} \tilde{G}_a^{\mu\nu} + \text{h.c.}$$

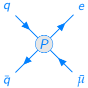

pseudoscalar

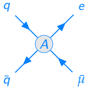

axialvector

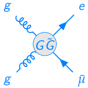

gluonic

Decay $P \to \bar{\mu} e$:

Decay Rate =

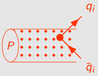

hadronic matrix elements

⊗

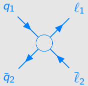

(short distance) EFT operator

SD $\mu \to e$ conversion:

Conversion Rate =

bound state physics

⊗

nuclear response

⊗

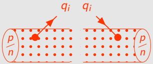

hadronic matrix elements

⊗

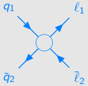

(short distance) EFT operator

Can use $\mu \to e$ conversion limits to derive limits on $P \to \bar{\mu} e$

Master Formula: $P \to \bar{\mu} e$

Decay Rate =

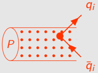

hadronic matrix elements

$\otimes$

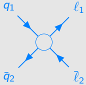

(short distance) EFT operator

$$\mathrm{Br}_{P\to\mu^\mp e^\pm} = \frac{(M_P^2 - m_\mu^2)^2}{16\pi\Gamma_P M_P^3} \sum_{Y=L,R} |C_Y^P|^2$$

$$C_Y^P = \sum_q \frac{b_q}{\Lambda^2}\left(\pm C_Y^{A,q} f_P^q m_\mu - C_Y^{P,q} \frac{h_P^q}{2m_q}\right) + \frac{4\pi}{\Lambda^3} C_Y^{G\tilde{G}} a_P$$

- only contributions from:

  $P, \quad A, \quad G\tilde{G}$

- hadronic matrix elements from lattice-QCD and phenomenology
- Ward identity:

  $$b_q f_P^q M_P^2 = b_q h_P^q - a_P$$

	π	η		η'	
		Pheno	Lattice	Pheno	Lattice
$\frac{b_u f_P^u}{F_\pi}$	1	0.80	0.77	0.66	0.56
$\frac{b_d f_P^d}{F_\pi}$	−1	0.80	0.77	0.66	0.56
$\frac{b_s f_P^s}{F_\pi}$	0	−1.26	−1.17	1.45	1.50
a_P [GeV^3]	0	–	−0.017	–	−0.038
a_P^{FKS} [GeV^3]	0	−0.022	−0.021	−0.056	−0.048
h_P^q	Ward identity				

Phenomenology: [Escribano et al., 2016]
Lattice-QCD: [Bali et al., 2021]

Master Formula: SD $\mu \to e$ conversion

Conversion Rate =  ⊗  ⊗ 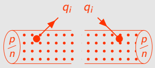 ⊗ 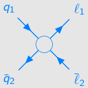

bound state physics — nuclear response — hadronic matrix elements — (short distance) EFT operator

$$\mathrm{Br}^{\mathrm{SD}}_{\mu\to e} = \frac{4m_\mu^5\alpha^3 Z^3}{\pi\Gamma_{\mathrm{cap}}(2J+1)}\left(\frac{Z_{\mathrm{eff}}}{Z}\right)^4 \times \sum_{\substack{Y=L,R\\ \tau=\mathcal{L},\mathcal{T}}}\left[C_Y^{\tau,00}S_{00}^{\tau} + C_Y^{\tau,11}S_{11}^{\tau} + C_Y^{\tau,01}S_{01}^{\tau}\right]$$

$$C_Y^{\mathcal{T},ij} = \left[\bar{C}_Y^{A,i}(1+\delta')^i \pm 2\bar{C}_Y^{T,i}\right]\times(i\leftrightarrow j); \quad C_Y^{\mathcal{L},ij} = \left[\bar{C}_Y^{A,i}(1+\delta'')^i - \frac{m_\mu}{2m_N}\bar{C}_Y^{P,i} \pm 2\bar{C}_Y^{T,i}\right]\times(i\leftrightarrow j)$$

$$\bar{C}_Y^{P,N} = \frac{1}{\Lambda^2}\sum_q C_Y^{P,q}\frac{m_N}{m_q}g_5^{q,N} - \frac{4\pi}{\Lambda^3}C_Y^{G\tilde{G}}\tilde{a}_N; \quad \bar{C}_Y^{A,N} = \frac{1}{\Lambda^2}\sum_q C_Y^{A,q}g_A^{q,N}; \quad \bar{C}_Y^{T,N} = \frac{1}{\Lambda^2}\sum_q C_Y^{T,q}f_{1,T}^{q,N}$$

- numerical solution of Dirac equation:
  $Z_{\mathrm{eff}}^{\mathrm{Al}} = 11.64, \qquad Z_{\mathrm{eff}}^{\mathrm{Ti}} = 17.65$ [Kitano et al., 2002]
- corr. from NLO chiral EFT and 2-body currents: $\delta' = -0.28(5), \quad \delta'' = -0.44(4)$
  [Hoferichter et al., 2020]

$g_A^{u,p}$	$g_A^{d,p}$	$g_A^{s,N}$	$\tilde{a}_N$ [GeV]	$g_5^{q,N}$
0.842(12)	-0.427(13)	-0.085(18)	-0.39(12) $[N_C\to\infty]$	Ward identity

[HERMES, 2007]

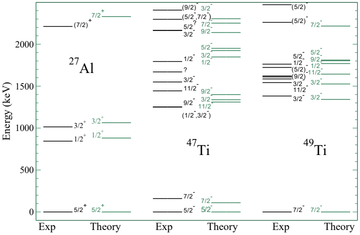

shell-model

Outlook: Full Masterformula for $\mu \to e$ conversion

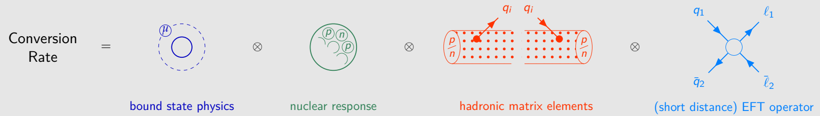

- effective Lagrangian with all possible quark and gluon operators:

$$\Gamma \in S, P, V, A, T, D, GG, G\tilde{G}$$

- hadronic matrix elements (including higher order terms): $F^{\Gamma,i}_{q,N}$
- nuclear multipoles (beyond SD and SI):

$$\mathcal{S} \in M, \Sigma^{(\prime\prime)}, \Phi^{(\prime\prime)}, \Delta^{(\prime\prime)}, \Omega^{(\prime\prime)}, \ldots$$

- full numerical solution of muon and electron wave functions

$$\mathcal{M} \sim \int \frac{\mathrm{d}^3 q}{(2\pi)^3} \sum_{\Gamma,q,i,N,\mathcal{S}} K^{\Gamma,i,\mathcal{S}_N}_{q,N}(\vec{q}) \cdot C^{\Gamma}_{q} \cdot F^{\Gamma,i}_{q,N}(\vec{q}) \cdot \mathcal{F}^{\mathcal{S}_N}(\vec{q}) \cdot \overbrace{\overline{\Psi}_e \mathcal{O}_\Gamma \Psi_\mu}(\vec{q})$$

Deduced Limits (individual)

- Use limits on $\mu \to e$ conversion to derive limits on $P \to \bar{\mu} e$

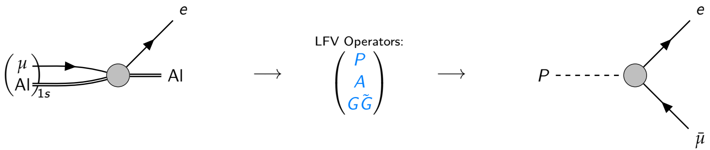

- In general the operators do not appear in the same linear combinations
- If we consider one operator at a time, the transition is immediate:

$\mu \to e$ (exp.)	$P \to \bar{\mu} e$ (derived)	current limit
$\mathrm{BR}_{\mathrm{Ti}} < 6.1 \times 10^{-13}$	$\mathrm{BR}_{\pi^0} \lesssim 4 \times 10^{-17}$	$< 3.6 \times 10^{-10}$
	$\mathrm{BR}_{\eta} \lesssim 5 \times 10^{-13}$	$< 6.0 \times 10^{-6}$
	$\mathrm{BR}_{\eta'} \lesssim 7 \times 10^{-14}$	$< 4.7 \times 10^{-4}$

(scan over all "one operator at a time"-scenarios and choices for constants)

Derived limits are several orders of magnitude better!

Deduced Limits (rigorous)

For rigorous limits we need to scan over all Wilson coefficients:

- Maximise: $$\frac{\Gamma_{P\to\bar{\mu}e}(C_P, C_A, C_{G\tilde{G}})}{\Sigma_{\mu\to e}(C_P, C_A, C_{G\tilde{G}})}$$
  $\to \exists$ fine-tuned solution: $\Sigma_{\mu\to e} \overset{!}{=} 0$
- In this scenario $\Gamma_{\pi^0\to\bar{\mu}e}$ vanishes as well:

rigorous limit: $\text{Br}_{\pi^0\to\bar{\mu}e} < 1.0 \times 10^{-13}$ $\left(\text{exp: } < 3.6 \cdot 10^{-10}\right)$

- However, $\Gamma_{\eta^{(\prime)}\to\bar{\mu}e}$ can still be non-zero:
  $\to \text{Br}_{\eta^{(\prime)}\to\bar{\mu}e}$ with sufficient fine-tuning in principle unbound
- easily spoilt by RG corrections
- contributing to SI $\mu \to e$ conversion

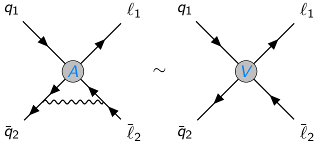

How to describe elastic electron scattering?

Typical description via Plane Wave Born Approximation

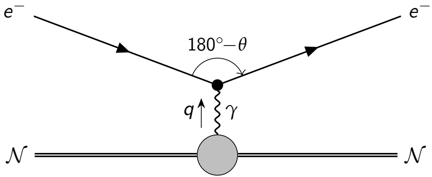

$$\frac{d\sigma}{d\Omega} = \left(\frac{d\sigma}{d\Omega}\right)_{\text{Mott}} \times \frac{E_e'}{E_e} \times \left|F(q,\theta)\right|^2$$

$$\left|F(q,\theta)\right|^2 = \sum_{\substack{L\,\text{even}\\ \leq 2J}} \left|ZF_L^{\text{ch}}(q)\right|^2 + \left(\tfrac{1}{2} + \tan^2\tfrac{\theta}{2}\right) \sum_{\substack{L\,\text{odd}\\ \leq 2J}} \left|F_L^{\text{mag}}(q)\right|^2$$

$J = 0$:

$$F(q,\theta) = ZF_0^{\text{ch}}(q) \overset{F.T.}{\longleftrightarrow} \rho_0(r)$$

- strongly dominating
- defines charge density

$J > 0$:

$$F(q,\theta) \supset F_{L>0}^{\text{ch}}, F_L^{\text{mag}}$$

- become relevant where F_0^{ch} small (zeroes, high q, high θ)
- subtract before extraction

Even for $J = 0$ insufficient $\rightarrow$ Coulomb corrections

Phase-shift model

- Born approximation assumes plane waves
- Finite extend of the nucleus distorts wave functions
- Employ numerical solutions:

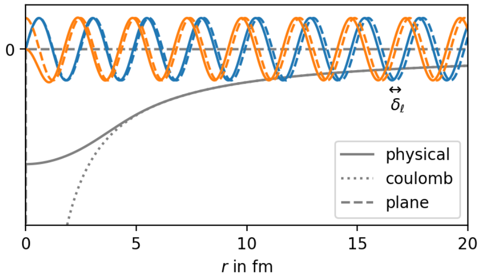

$$F_0^{\text{ch}}(q) \overset{F.T.}{\longleftrightarrow} \rho_0(r) \rightarrow \underbrace{V(r) \xrightarrow{\text{Dirac-eq.}} \psi^{(e)}_{\text{in/out}}(r,\theta) \rightarrow \frac{d\sigma}{d\Omega}}_{\text{phase-shift model}}$$

phase-shift model: Solve Dirac-eq. $\forall_\ell$: $\left[\psi_\ell \sim \begin{pmatrix} g_\ell(r) \\ i f_\ell(r) \end{pmatrix} \rightarrow \delta_\ell = \delta_\ell^C + \bar{\delta}_\ell\right]$

$$\Rightarrow \frac{d\sigma}{d\Omega} \sim \left(1+\tan^2\left(\frac{\theta}{2}\right)\right)|f(\theta)|^2 \quad \text{with} \quad f(\theta) \sim \sum_\ell P_\ell(\cos(\theta))e^{2i\delta_\ell}$$

Ab initio inputs

^{27}Al ($J = \frac{5}{2}$) requires $L > 0$ contributions

ZF_L^{ch} $\quad$ F_L^{mag}

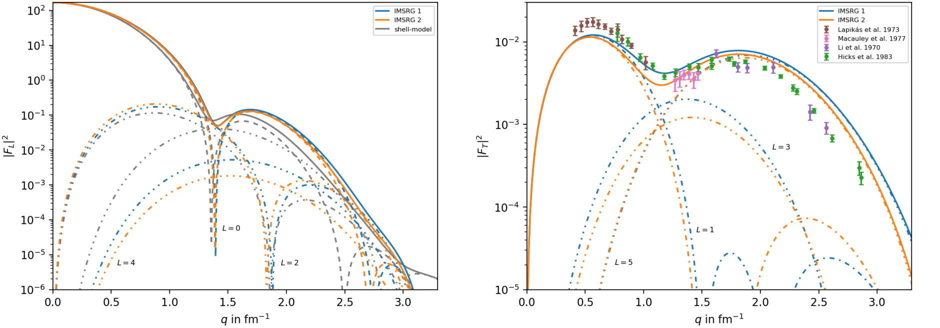

- Subtract and remove data points dominated by $L > 0$
- So far: No Coulomb corrections for $L > 0$ (requires DWBA)

Charge density results

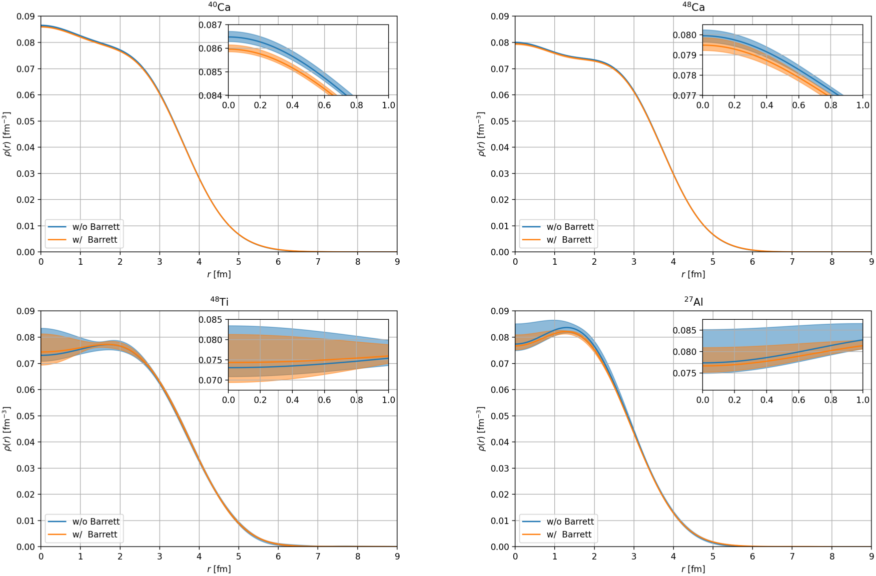

Radii

- Qualitative radii for the considered nuclei
- Statistical uncertainties
  - based on fit statistics and data uncertainties
- Systematical uncertainties
  - based on different R, N with two strategies

All parameterizations with uncertainties and correlations are made available in a complementary python notebook

Nucleus	$\sqrt{\langle r^2 \rangle}$ [fm]	Refs.
^{27}Al	$2.996(11)\,{}^{(43)[44]}_{(^{+26}_{-33})[35]}$	3.035(2)
	$3.063(3)\,{}^{(30)[31]}_{(^{+0}_{-1})[3]}$	3.0610(31)
^{40}Ca	$3.452(3)\,{}^{(8)[9]}_{(^{+1}_{-9})[10]}$	3.450(10)
	$3.4771(17)\,{}^{(17)[24]}_{(^{+0}_{-5})[17]}$	3.4776(19)
^{48}Ca	$3.4499(29)\,{}^{(31)[42]}_{(^{+42}_{-52})[60]}$	3.451(9)
	$3.475(2)\,{}^{(10)[10]}_{(^{+0}_{-3})[4]}$	3.4771(20)
^{48}Ti	$3.62(3)\,{}^{(8)[8]}_{(^{+2}_{-3})[4]}$	3.597(1)
	$3.596(3)\,{}^{(57)[57]}_{(^{+1}_{-1})[3]}$	3.5921(17)

Shell model spectrum

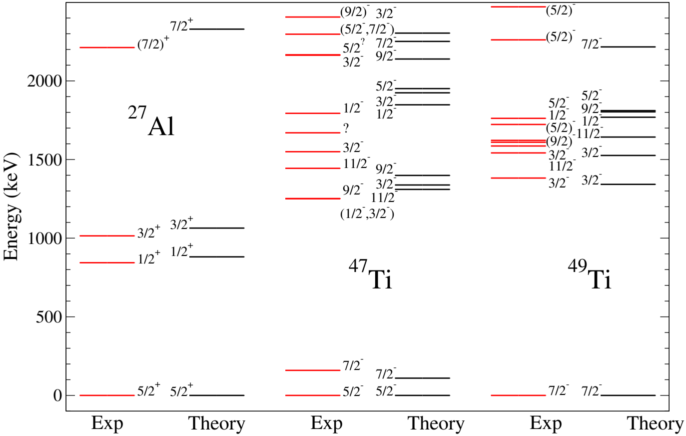

Formulas I

$$\langle 0|\bar{q}\gamma^{\mu}\gamma_5 q|P(k)\rangle = i b_q f_P^q k^{\mu}, \tag{1}$$

$$\langle 0|m_q \bar{q} i\gamma_5 q|P(k)\rangle = \frac{b_q h_P^q}{2}, \tag{2}$$

$$\langle 0|\frac{\alpha_s}{4\pi} G_{\mu\nu}^a \tilde{G}_a^{\mu\nu}|P(k)\rangle = a_P, \tag{3}$$

$$\langle N|\bar{q}\gamma^{\mu}\gamma_5 q|N\rangle = g_A^{q,N}\langle N|\bar{N}\gamma^{\mu}\gamma_5 N|N\rangle, \tag{4}$$

$$m_q\langle N|\bar{q} i\gamma_5 q|N\rangle = m_N g_5^{q,N}\langle N|\bar{N} i\gamma_5 N|N\rangle, \tag{5}$$

$$\langle N|\bar{q}\sigma^{\mu\nu} q|N\rangle = f_{1,T}^{q,N}\langle N|\bar{N}\sigma^{\mu\nu} N|N\rangle, \tag{6}$$

$$\langle N|\frac{\alpha_s}{4\pi} G_{\mu\nu}^a \tilde{G}_a^{\mu\nu}|N\rangle = \tilde{a}_N\langle N|\bar{N} i\gamma_5 N|N\rangle, \tag{7}$$

Formulas II

$$\mathrm{Br}_{\mathrm{SI}}[\mu \to e] = \frac{4m_\mu^5}{\Gamma_{\mathrm{cap}}} \sum_{Y=L,R} \left| \sum_{\substack{N=p,n \\ \mathcal{O}=S,V}} \bar{C}_Y^{\mathcal{O},N} \mathcal{O}^{(N)} \right|^2, \tag{8}$$

$$\bar{C}_Y^{S,N} = \frac{1}{\Lambda^2} \sum_q C_Y^{S,q} \frac{m_N}{m_q} f_q^N + \frac{4\pi}{\Lambda^3} C_Y^{GG} a_N, \tag{9}$$

$$\bar{C}_Y^{V,N} = \frac{1}{\Lambda^2} \sum_q C_Y^{V,q} f_{V_q}^N, \tag{10}$$

$$S^{(N)} = V^{(N)} = \frac{(\alpha Z)^{3/2}}{4\pi} \left(\frac{Z_{\mathrm{eff}}}{Z} \right)^2 \mathcal{F}_N^M(m_\mu^2), \tag{11}$$

Formulas III

$$\bar{C}^0 = \frac{\bar{C}^p + \bar{C}^n}{2}, \qquad \bar{C}^1 = \frac{\bar{C}^p - \bar{C}^n}{2}, \tag{12}$$

$$g_A^{q,N} = g_5^{q,N} - \frac{\tilde{a}_N}{2m_N}, \tag{13}$$

$$\tilde{a}_N = -2m_N g_A^{u,0} = -0.39(12)\ \mathrm{GeV}, \tag{14}$$

Formulas IV

$$C_Y^{A,u} = C_Y^{A,d}, \qquad C_Y^{A,s} = -\frac{2\,C_Y^{A,u} g_A^{u,0}}{g_A^{s,N}}, \tag{15}$$

$$\frac{C_Y^{P,u}}{m_u} = \frac{C_Y^{P,d}}{m_d}, \qquad \frac{C_Y^{P,s}}{m_s} = \frac{4\pi}{\Lambda} C_Y^{G\tilde{G}} \frac{2 g_A^{u,0}}{g_A^{u,0} - g_A^{s,N}}. \tag{16}$$

Formulas V

$$S_{00}^{\mathcal{T}} = \sum_L \left[\mathcal{F}_+^{\Sigma'_L}(q^2)\right]^2, \qquad S_{00}^{\mathcal{L}} = \sum_L \left[\mathcal{F}_+^{\Sigma''_L}(q^2)\right]^2, \tag{17}$$

$$S_{11}^{\mathcal{T}} = \sum_L \left[\mathcal{F}_-^{\Sigma'_L}(q^2)\right]^2, \qquad S_{11}^{\mathcal{L}} = \sum_L \left[\mathcal{F}_-^{\Sigma''_L}(q^2)\right]^2, \tag{18}$$

$$S_{01}^{\mathcal{T}} = \sum_L 2\mathcal{F}_+^{\Sigma'_L}(q^2)\,\mathcal{F}_-^{\Sigma'_L}(q^2), \tag{19}$$

$$S_{01}^{\mathcal{L}} = \sum_L 2\mathcal{F}_+^{\Sigma''_L}(q^2)\,\mathcal{F}_-^{\Sigma''_L}(q^2), \tag{20}$$

Table

	π^0	η	η'
$C_Y^{A,3}$	1.3×10^{-17}	–	–
$C_Y^{A,8}$	–	1.5×10^{-17}	4.0×10^{-20}
$C_Y^{A,0}$	–	2.9×10^{-19}	2.1×10^{-19}
$C_Y^{P,3}$	4.1×10^{-17}	–	–
$C_Y^{P,8}$	–	1.6×10^{-12}	2.1×10^{-14}
$C_Y^{P,0}$	–	4.1×10^{-12}	5.4×10^{-13}
$C_Y^{G\tilde{G}}$	–	5.8×10^{-15}	4.7×10^{-16}